THE FOM-MEQALAC SYSTEM: THE RF ACCELERATOR

R.W. Thomae, F. Siebenlist, P.W. van Amersfoort, E.H.A. Granneman,
FOM-Institute for Atomic and Molecular Physics,
Kruislaan 407, 1098 SJ Amsterdam, The Netherlands

H. Klein, A. Schempp, T. Weis
Institut für Angewandte Physik, University Frankfurt
Robert-Mayerstrasse 2-4, 6000 Frankfurt/M, FRG

Summary

In MEQALAC systems a large number of small, parallel beamlets is accelerated simultaneously. We present a compact system in which four He^+ beams are to be accelerated from 40 to 115 keV. It is based on a modified Interdigital H resonator (TE 111). The length and the diameter of the 40 MHz resonator are 0.65 and 0.40 m, respectively. In between the 20 acceleration gaps quadrupole lenses are placed to ensure radial stability of the beam. Calculations have been performed to find conditions for stable acceleration. The theoretical (average) space charge limited current is ~3 mA/channel. Parameters are given of a 100 mA, 6 MeV Li^- accelerator to be used for plasma diagnostics.

Introduction

At low particle energies ($\lesssim$50 keV/N) the space charge loading of the beam sets severe limits to the current which can be transported and accelerated. A possible way to overcome this problem is to use a MEQALAC system (Multiple Electrostatic Quadrupole Array Linear ACcelerator, after Maschke[1]), in which instead of a single beam a large number of small parallel beamlets is accelerated simultaneously by means of RF fields. Strong focusing electrostatic quadrupole lenses are placed in between the acceleration gaps to prevent space charge induced blow-up of the beam and to counteract the radial defocusing effect of the accelerating field.

The advantage of a system like this is that in principle an arbitrarily large current can be accelerated, just by increasing the numbers of beamlets.

To investigate the properties of such a MEQALAC system we developed a 40 MHz Interdigital H resonator for the acceleration of four He^+ beams with average current of ~3 mA/channel from 40 to ~115 keV. In the following sections of the paper we present a short description of the experimental setup and preliminary results of the low level measurements made on the RF resonator. At the end parameters are given for a 100 mA, 6 MeV Li^- accelerator.

Experimental setup

A schematic picture of the FOM experiment is shown in fig. 1.

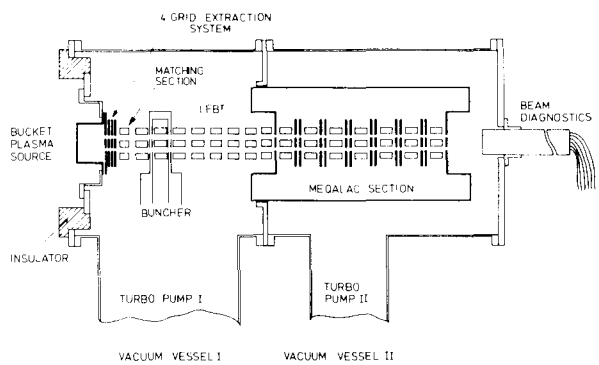

Fig. 1. The experimental set-up. For details, see text.

From a bucket ion source four He^+ beams are extracted. A low energy beam transport section (LEBT) transports the ions from the high pressure ion source region to the low pressure RF acceleration region. The first five lenses can be tuned individually to match the cylindrically symmetric beam coming out of the source to the periodic focusing system of the LEBT and MEQALAC sections. Halfway the LEBT section the DC beams are bunched by means of a two-gap buncher and subsequently injected into the MEQALAC accelerator[2,3,4,8].

Description of the resonator

It was decided to use a modified version of the Interdigital H resonator (TE 111 mode)[9]; the resonator is shown schematically in fig. 2.

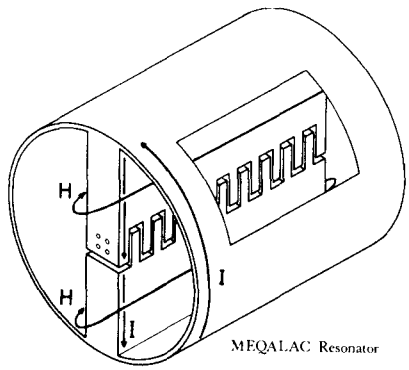

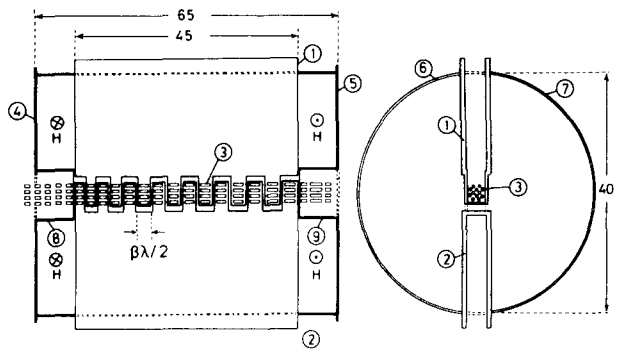

Fig. 2. The MEQALAC accelerator structure. The resonator is a modified Interdigital H resonator. The number of gap is 20. For simplicity fewer gaps are shown. The gaps are water cooled (not shown in picture). All dimensions are in cm.

On opposite sides of a cylindrical cavity two hollow rectangular boxes (1,2) are mounted. These have a rectangular, fingerlike structure on the side pointing inwards. On the axis the two fingerstructures face each other, in that way forming 20 acceleration gaps. Inside the fingers the quadrupole elements (3) are mounted. The side of the boxes sticking out of the cavity is open and allows for adequate pumping of the quadrupole area. Through these open ends water cooling is brought into the RF gaps and also the electrical leads feeding the quadrupoles. In this way the leads and the quadrupoles are fully shielded from the RF field except for a small leakage through the beam holes.

When the cylindrical ground mode (TE 111) is excited in the cavity the RF current flows as indicated in fig. 2. The RF potential difference present between top and bottom of the cylinder is thus used to generate a longitudinal electric field on axis. The magnetic field flows around the boxes. Because it must have space to turn around, the end plates (4,5) closing the resonator are located at a distance of ~10 cm from the short sides

of the boxes. The beams enter and leave the resonator through two inserts (8,9) which allow them to propagate in a (RF) field free space up to the first accelerator gap and from the last acceleration gap onwards.

Voltage distribution

To investigate the properties of this resonator the fingerstructure was simulated by an array of separate solid copper blocks in which 4 "beam" holes are drilled. By adjusting the position of the blocks the gap widths and with that the resonator capacitance C_{RES} is varied. To study the influence of the shape of the blocks two different types were examined. In the first structure (type I) the width of the blocks and the capacitance per cell is kept constant. In the second structure (type II) the capacitance per unit length is kept constant. This is realized by increasing the width of the blocks proportionally with the anticipated particle velocity. The axial distribution of the electric field is obtained by pulling a small perturbation ball (bronze, $\emptyset = 2$ mm) through the gaps and measuring the resulting frequency shift. In figure 3a the mean voltage <U> across the gaps for the two structure types are shown.

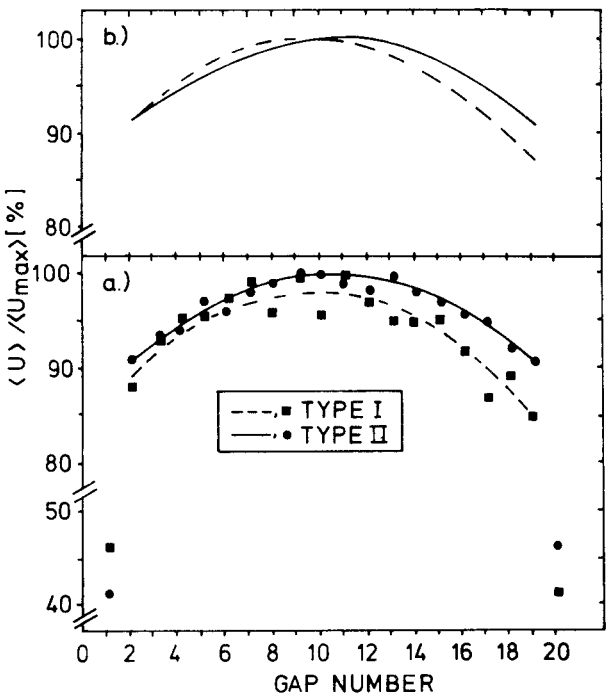

Fig. 3. a) The mean voltage across the gaps normalized to the maximum value. The dots indicate mean values for measurements done at different gap widths.
b) The (mean) curves are normalized to values of 100%.

The gap to gap variation can possibly be explained by differences in the contact resistances between blocks and support or by radial displacement of some of the blocks. This causes the perturbation ball to travel closer to the aperture edge, thereby sampling a higher field. In fig. 3b the maximum of the two lines is normalized to 100% to allow a comparison between the structures. For the type II structure (constant capacitance per unit length) we measured a symmetric voltage distribution with respect to the central peak (gap 10). The voltage drop at the beginning (2) and the end (19) of the structure is 9%. The field strength in gaps 1 and 20 is roughly half of that in the rest of the gaps. Since for type I structure the capacitance per unit length decreases with increasing $\beta\lambda/2$ (cell length), this voltage drop is enhanced at the high energy end of the resonator ($<U>/<U_{MAX}> \approx 14\%$). To characterize the degree of unflatness, we define a parameter

$$\alpha = \sum_{i=1}^{n} \frac{U_i}{U_{MAX}} \cdot \frac{1}{n} \qquad (1)$$

For the two structures: $\alpha_I = 0.89$; $\alpha_{II} = 0.91$.

Resonator reactances and resonance frequency

The total resonator capacitance C_{RES} is the sum of the gap capacitances and the stray capacitances. For the examined gap distances ($1.3\ mm \leq d \leq 2.3\ mm$) the structure capacitance is about 95% of the total resonator capacitance. In fig. 4a the resonance frequency is shown as a function of the gap distance and the total resonator capacitance C_{RES}. For the required resonance frequency of 40 MHz C_{RES} is of the order of 350 pF. The resonator inductance can roughly be determined from:

$$L_{RES} \approx \frac{\mu_0 F_L}{\bar{\ell}} \qquad (2)$$

in which μ_0 is the magnetic permeability, F_L is the half cross section of the resonator and $\bar{\ell}$ the mean path length around the meander structure. For the dimensions of the MEQALAC resonator (2) leads to $L_{RES} = 46$ nH.

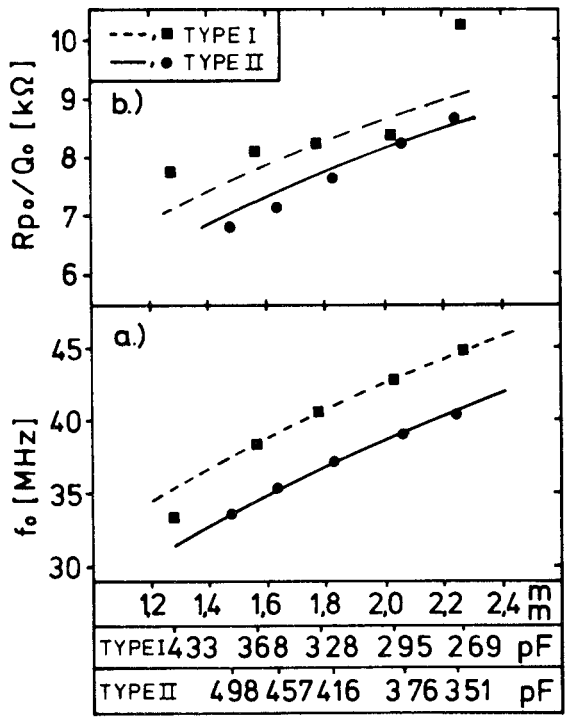

Fig. 4. a) The resonance frequency f_0 as a function of the gap width d and the resonator capacitance C_{RES}. The lines give the theoretical dependence $f_0 = 1/(4\pi^2 C_{RES} L_{RES})^{\frac{1}{2}}$.
b) The R_{po}/Q_0 values for the two structures as a function of the gap distance d. The curves give the theoretical dependence according to (4).

Resonator shunt impedance and quality

By means of the perturbation ball method the ratio of the resonator shunt impedance R_{po} and resonator quality factor Q_0 was determined.

$$\frac{R_{po}}{Q_0} = \frac{(\int E\,dz)^2}{\omega_0 W} \qquad (3)$$

E is the electric field on axis, ω_0 the (angular) resonance frequency and W the stored energy in the resonator. (3) can be calculated[5] according to:

$$\frac{R_{po}}{Q_o} = \frac{F_L \mu_o \gamma_o}{\pi^2 (\beta c)^2} \cdot C_{RES}^{-3/2} \qquad (4)$$

βc is the particle velocity, and

$$\gamma_o = (\int_o^L I_\phi \, dz/L)^2 / \int_o^L I_\phi^2 \, dz/L,$$

where I_ϕ is the azimuthal current and L the length of the resonator. From fig. 3 we find:

$$\gamma_{o_I} = 0.80; \quad \gamma_{o_{II}} = 0.81.$$

It is assumed that before gap 1 and beyond gap 20 I_ϕ drops linearly to zero over the distance of 10 cm to the end walls. In fig. 4b the results of the measurements and the theoretical dependence are given for both structures. For a resonance frequency of 40 MHz the R_{po}/Q_o values are of the order of 8 kΩ. The measured Q_o values are $1000 \leq Q_o \leq 1400$. For the final fingerstructure which is machined from one peace d = 2 mm was chosen (40 MHz); a R_{po} value ≥ 15 MΩ is expected. This means that four 40 keV beams with an average current of 3 mA/channel can be accelerated to 115 keV with an efficiency ≈60% (conversion of RF power into particle power). In table I a list of the characteristic parameters of the accelerator is presented. In fig.5 a photo of the resonator is shown.

A 6 MeV Li^- accelerator

Based on our prototype experience we scaled the present system up to a high energy, high power system. In table I a design of a 6 MeV, 100 mA Li^- accelerator is given. With this accelerator a 6 MeV Li° beam can be produced; such a beam can be used to determine the alpha-particle energy distribution of a fusion plasma[7]. The accelerator is made up of two stages. In the second stage the resonance frequency is twice of that in the first stage. The acceleration efficiency is 67%. The total length of the system is 6.2 m. By increasing the injection energy or the number of channels the total accelerated current can be scaled up to higher values (with similar efficiencies).

Conclusions

Studies of a MEQALAC accelerating system show that a system can be built with a high accelerating efficiency (65%). This is better than that obtained with other low β structures (20% - 50%)[6]. Field measurements confirm for both investigated structures that the voltage distribution in the TE 111 cavity is sufficiently flat. The 40 MHz resonator is compact. Future beam acceleration tests have to show its performance at high power levels.

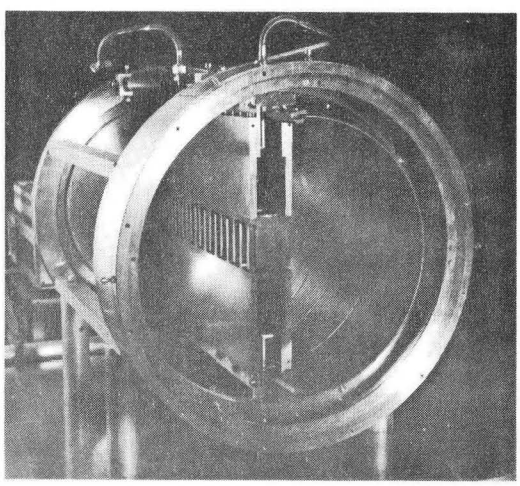

Fig. 5. The MEQALAC resonator with the final fingerstructure (type I). Only one of the two half-cylinder copper shells is mounted.

TABLE I

Parameter	Present exp.	Li accelerator stage 1	stage 2	Dim.
Particle	He^+	$^6Li^-$	$^6Li^-$	
Inj.energy	40	90	1210	keV
Exit energy	115	1210	6010	keV
RF frequency	40	40	80	MHz
Synchr.phase	-38	-33	-16	°
Trans.time factor	0.9	0.9	0.9	
Gap elec.field	2.6	9.3	8.0	MV/m
Av.acc.el.field	0.1	0.4	1.35	MV/m
Nr.of gaps	20	41	49	
Nr.of channels	4	16	16	
Overall beam dim.	4	25	25	cm^2
Length resonator	65	260	355	cm
Diam.resonator	40	65	65	cm
Capacitive load (AV.)	7.0	2.6	0.7	pF/cm
Qual.factor Q_o	1800	2900	4100	
Shunt imped.R_{po}	16	44	120	MΩ
$R_{po,eff}$	9	26	91	MΩ
RF power losses	0.5	5.0	6.3	cm
(AV.)cell length	2.3	5.0	6.3	cm
Width RF gaps	0.2	0.4	1.3	cm
Quad.space/length	0.75	0.75	0.8	
Diam.quad.chan.	0.6	0.6	0.6	cm
Quad.voltage	±2.62	±4.09	±5.97	kV
Zero current μ_{oT}	60	80	20	°
Zero current μ_{oL}	20.0	34.5	10.6	°
Depressed μ_T	7.3	24.0	4.8	°
Depressed μ_L	8.0	10.4	6.7	°
Chan.acceptance α_T	108.π	83.π	26.π	mm.mrad
Chan.acceptance α_L	240.π	343.π	44.π	mm.mrad
$I_{T,MAX}$	24.1	59.8	151.0	mA
$I_{L,MAX}$	22.6	142.0	130.5	mA
$I_{T,AV}$	3.0	6.3	7.8	mA
$I_{L,AV}$	2.8	15.0	6.7	mA
Tot.current $I_{TOT,AV}$	11.2	101	101	mA
Acceler.efficiency	60	70	66	%

TABLE I. The characteristic parameters of two MEQALAC accelerators. In the first column the present He^+ system is given. In the second and third column a 100 mA, 6 MeV Li^- accelerator is presented. This accelerator consists of two stages. In the first stage acceleration takes place from 90 to 1210 keV; in the second stage to 6 MeV. The subscripts L and T denote the longitudinal and transverse dimensions, respectively; the subscripts MAX and AV for peak and average, respectively. μ is the phase advance per cell.

References

1 A.W. Maschke, Brookhaven Natl.Lab., report BNL-51209 (1979).

2 P.W. van Amersfoort, E.H.A. Granneman, J. Kistemaker, F. Siebenlist, R.W. Thomae, H. Klein, A. Schempp, FOM-report nr. 55.120, November 1982.

3 F. Siebenlist, R.W. Thomae, P.W. van Amersfoort, E.H.A. Granneman, J. Kistemaker, H. Klein, A. Schempp, FOM-report nr. 56.298, May 1983.

4 R.W. Thomae, P.W. van Amersfoort, F. Siebenlist, F.G. Schonewille, E.H.A. Granneman, J. Kistemaker, H. Klein, A. Schempp, T. Weis, FOM-report nr. 57.379, December 1983.

5 J. Pottier, IEEE Trans.Nucl.Sci., NS-16, No. 3, 372 (1969).

6 H. Klein, IEEE Trans.Nucl.Sci., NS-30, No. 4, 3313 (1983).

7 L.R. Grisham, D.E. Post, D.R. Mikkelsen, Nucl.Techn./Fusion, to be published; Princeton report: PPPL-1886.

8 F. Siebenlist, R.W. Thomae, P.W. van Amersfoort, E.H.A. Granneman, H. Klein, A. Schempp, T. Weis, these proceedings.

9 T. Weis, H. Klein, A. Schempp, these proceedings.